



Phase Transition, Molecular Polarizability and Histogram Equalization Studies on Two Liquid Crystals of Same Terminal Group and Different Linking and End Chains

Shobha N.C^{1*}, K. Fakkrudin², Anitha R³ and Swarna S⁴

¹Department of Physics, A.P.S. College of Engineering, Bengaluru – 560082, Karnataka, India.

²Department of Physics, Ghousia College of Engineering, Ramanagara– 562159, Karnataka, India.

³Department of Chemistry, K.S. School of Engineering & Management, Bengaluru – 560109, Karnataka, India.

⁴Department of Chemistry, K.S. School of Engineering & Management, Bengaluru – 560109, Karnataka, India

Received: 04 Aug 2023

Revised: 14 Aug 2023

Accepted: 07 Sep 2023

*Address for Correspondence

Shobha N.C.

Department of Physics,

A.P.S. College of Engineering,

Bengaluru – 560082, Karnataka, India,

E. Mail: shobhanishanth123@gmail.com



This is an Open Access Journal / article distributed under the terms of the **Creative Commons Attribution License** (CC BY-NC-ND 3.0) which permits unrestricted use, distribution, and reproduction in any medium, provided the original work is properly cited. All rights reserved.

ABSTRACT

The optical textures and Phase transition temperatures exhibited by liquid crystalline compounds viz 4-Cyano-4'-propoxy-1,1'-biphenyl and 6-Cyano-2-naphthyl 4-heptylcyclohexane carboxylate are recorded by Polarizing Optical Microscope (POM), for confirmation the phase transition temperatures are also estimated by (DSC) Differential Scanning Calorimeter. Using phase transition temperatures the molecular polarizabilities of the compounds are estimated by quantum dynamical method. A theoretical approach. The density and refractive indices are carried out. By density studies it is noticed that 4-Cyano-4'-propoxy-1, 1'-biphenyl compound exhibit only nematic phase and 6-Cyano-2-naphthyl 4-heptylcyclohexanecarboxylate exhibit nematic and smectic A phases. The refractive indices and density data is used to evaluate molecular polarizabilities by well known Vuk's and Neugabaur methods. The molecular polarizabilities are found to be same in theoretical and experimental methods. Histogram equalization technique is exploited on textural images to improve contrast in image.

Keywords: Density, Histogram, Liquid crystals, Phase transition, Polarizability, Refractive indices.





Shobha et al.,

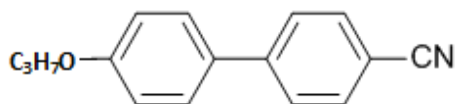
INTRODUCTION

The advent of the invention of Liquid Crystals, their use and potential application in display and memory devices made the Physicists, Chemists and technocrats to plunge into the liquid crystal field and contribute their respective might to show that these materials are potential candidates in industry. To utilize the liquid crystalline materials in display one ought to know the thermal, electrical, optical and dilatometric properties [1]. The information on the refractive indices and phase transitions are imperative to choose the materials for display technology and in photonics. The Liquid Crystalline state is characterized by the orientational ordering of the constituent molecules and transition between different mesophases. These transitions are usually marked by the changes in various anisotropic properties. Be that as it may, contingent on the order of the transition they may also be joined by changes in scalar quantities for example, enthalpy content or density [2]. The density studies involving temperature variation and across different phase transformations are for long known [3-7] to give information with respect to the nature of phase transition and growth of pretransitional effect. Further such investigations gives complimentary and confirmatory experimental evidence for the outcomes obtained using other techniques for example polarizing thermal microscope and differential scanning calorimetry(DSC) regarding the assurance of phase transition temperature and the thermal stability of the phase of interest.

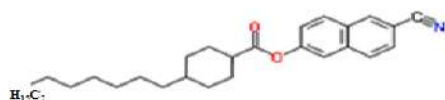
The most remarkable features of liquid crystals, crucial for their applications are anisotropic optical properties [8]. The refractive indices are one of the bulk tensorial properties which can be used to determine molecular polarizability and orientational order parameter. A uniaxial liquid crystal is birefringent. The temperature variation of birefringence is measured by using small angle prism and modified spectrometer. The molecular polarizability and Polarizability anisotropy are the important parameters of liquid crystals to evaluate the orientational order parameter, because the intermolecular interaction energies according to several theoretical models [8-13] are based on them. In the present studies the molecular polarizabilities of the liquid crystals are estimated by theoretical and experimental methods which are found to be same.

Usually the image will have poor contrast because most of the intensity values fit in narrow range. While managing discrete quantities we work with histograms. In general, the histogram of the refined image won't be uniform, because of discrete nature of the variables. Histogram equalization does out the intensity values of pixels in the input image such that the output image carry a uniform distribution of intensities. It improves the contrast and gets a uniform histogram. This technique can be used on an entire image or just on a fragment of image. The histogram equalization studies are done on the textural images. 4-Cyano-4'-propoxy-1, 1'-biphenyl is Procured by TCI Japan and 6-Cyano-2-naphthyl 4-heptylcyclohexanecarboxylate is procured by Frinton Laboratories, New Jersey, USA. The molecular structure of the liquid crystal is mentioned below.

1. 4-Cyano-4'-propoxy-1, 1'-biphenyl



2. 6-Cyano-2-naphthyl 4-heptylcyclohexanecarboxylate





Optical Textures

Polarizabilities by Theoretical Method

Lippincott δ Function Method

In crystalline state, there will be just the crystalline field acting on the system while in liquid phase, pure Brownian field just acts. Nonetheless, in liquid crystalline state, both these fields will be acting as this state will have the flow property like a liquid and anisotropic property like pure crystal. The resultant impact is the increase in the potential of the electron (system). As such, the shielding on the electrons will be less in this way adding to more polarization[20]. This conduct on account of liquid crystals can be expressed empirically as.

$$A_{LC} = A \exp [T - T_c] / T_c$$

Where T is the temperature relevant to the study of the liquid crystal property and T_c is the liquid crystalline transition temperature (clearing temperature), A and A_{LC} are the reduced electro negativities (REN) values in isotropic and LC phases. The molecular polarizability anisotropies can be obtained by the following expression.

$$\sum \alpha_{\parallel P} = \frac{4nA}{a_o} \left(\frac{R^2}{4} + \frac{1}{2c_R^2} \right) \left[e^{-\left[\frac{x_1 - x_2}{4} \right]^2} \right] \left(e^{\frac{T - T_c}{T_c}} \right)$$

$$\sum \alpha_{\parallel n} = \sum f_j \alpha_j$$

$$\sum 2\alpha_{\perp} = [3N - 2n_b] \left(\frac{\sum x_j^2 \alpha_j}{\sum x_j^2} \right)$$

Now the mean polarizability, α is given by

$$\alpha = \frac{\sum \alpha_{\parallel P} + \sum \alpha_{\parallel n} + \sum 2\alpha_{\perp}}{3}$$

Experimental

Thermal Microscopy

The liquid crystalline compounds are birefringent and shows optical textures[14 -15] for various thermotropic phases. A polarizing microscope SD TECHS-SDVPM2727 with the hot stage is used to distinguish different phases[16] and phase transition temperatures. An indigenous U-shaped bi-capillary Pyknometer in conjunction with the cathetometer was utilized for the density measurements.

Optical Birefringence Studies

The refractive indices of the liquid crystals are estimated with wedge shaped glass cell, like the one used to obtain birefringence by Haler et al[11] with a changed spectrometer. A wedge shaped glass cell was formed with two optically level rectangular glass plates (50mmx25mm) sandwiched with glass plate (0.4mm) which goes about as a wedge spacer. The optical flats are uniformly rubbed along the short edge to get the alignment of the LC molecule. The cell is filled with the LC material. The LC in the cell goes about as a uniaxial crystal with its optic axis parallel to the edge of the spacer glass plate.

Refractive Indices

Estimation of molecular polarizability by Vuks & Neugebauer model - Experimental

For the calculation of the molecular polarizabilities of LC molecules, the author has considered Vuks model which considers the nearby field of the molecule is isotropic and Neugebauer model which considers the nearby field as anisotropic. The applicable conditions of the two models for the estimation of molecular polarizabilities are given underneath.

Vuks Method

This model was first applied to LC molecules by Chandrasekhar et al[17]. assuming the internal field is isotropic even in anisotropic crystal. These assumptions lead to the following equations.





Shobha et al.,

$$\alpha_e = \left[\frac{3}{4\pi N} \right] \left[\frac{n_e^2 - 1}{n + 2} \right]$$

$$\alpha_o = \left[\frac{3}{4\pi N} \right] \left[\frac{n_o^2 - 1}{n + 2} \right]$$

Where N is the number of molecules per unit volume, ne & no are the extraordinary & ordinary refractive indices of the LC molecule.

$$n = \left[\frac{n_e^2 + 2n_o^2}{3} \right]$$

$N = \frac{N_A \rho}{M}$ where NA is the Avogadro number, M is the molecular weight and ρ is the density.

Neugebauer method

Subramanyam and Krishna murthy *et al* [18]. put in this procedure to LC molecule. In accordance with this method the molecular polarizabilities are

$$\alpha_e = \left(AB - 3 \pm \sqrt{(AB - 3)^2 - 4AB} \right) / 2A$$

$$\alpha_o = \left(AB + 3 \pm \sqrt{(AB + 3)^2 - 16AB} \right) / 4A$$

where

$$A = \frac{1}{\alpha_e} + \frac{2}{\alpha_o} = \frac{4\pi N}{3} \left[\frac{n_e^2 + 2}{n_e^2 - 1} \right] + \left[\frac{2(n_o^2 + 2)}{n_o^2 - 1} \right]$$

$$B = (\alpha_{||} + 2\alpha_{\perp}) = (\alpha_e + 2\alpha_o) = 3\alpha = 9 \left(\frac{n^2}{n - 1} \right) / \left[(4\pi N_i) \left(\frac{n^2}{n + 2} \right) \right]$$

Ni is the number of molecules per unit volume in the isotropic phase

Histogram equalization

For true implementation of histogram equalization the following procedure is used. Let Pr (rj), j= 1,2,...,L, means the histogram related with the intensity levels of a given image and review that the values in a normalized histograms are approximations to the probability of occurrence of each intensity level in the image. For discrete amounts we work with summations and the equalization transformation becomes[19]

$$\begin{aligned} S_k &= T(r_k) \\ &= \sum_{j=1}^k Pr(r_j) \\ &= \sum_{j=1}^k \left(\frac{n_j}{n} \right) \end{aligned}$$

For k = 1,2,...,L, where it is the intensity value in the output image corresponding to value rk in the input image.

Histogram equalization is executed by X=histequ(I , LEV)





Shobha et al.,

Where I is the input image, and LEV is the quantity of intensity levels determined for the output image. On the offchance that LEV is equal to 'L' i.e., the total number of possible levels in the input image, then histogram equalization implements the transformation function, $T(r_k)$, directly. If LEV is less than 'L', then histogram equalization attempts to distribute the levels so that they will approximate a flat histogram. The default value in histogram equalization is $LEV = 64$. For the most part, we use the maximum possible number of levels (i.e., 256) for LEV because this produces a true implementation of the histogram equalization method.

Histogram Figures

RESULTS AND DISCUSSIONS

Phase Transitions

The transition temperatures measured in the two crystalline compounds are introduced in table 1. Both compounds exhibit characteristic optical textures. The compound 4-Cyano-4'-propoxy-1, 1'-biphenyl exhibit monovariant nematic phase, whereas 6-Cyano-2-naphthyl 4-heptylcyclohexanecarboxylate exhibit nematic and SmA phases. Phases are related to the standard textures obtained using polarizing microscope connected with hot stage. The temperature variation of density is estimated in compound 1 and 2 and illustrated in figures 3 and 4. The essence of phase transitions concentrated through Dilatometry shows nematic and SmA phases. The density estimation are useful in deciding the order of phase transitional, pre transitional behavior. The first order phase transitional is characterized by sharp change in specific volume related with a thermal expansion coefficient. It is found that density diminishes with the increment of temperature in liquid crystalline phases except in the vicinity of a phase transformations where it shows a sharp increment before it accomplishes equilibrium value of next phase.

The density hop $\left[\frac{\Delta\rho}{\rho}\right]$ is determined as the vertical distance between density values ρ_1 and ρ_2 obtained by linear extrapolation density values, observed density jump, thermal expansion coefficient and density slope across different phases are represented in table 3. The slope of density variation in 4-Cyano-4'-propoxy-1, 1'-biphenyl is $1.73 \times 10^{-4} \text{C}^{-1}$ in isotropic nematic transition and $5 \times 10^{-4} \text{C}^{-1}$ in nematic crystal transition. The higher value of slope in nematic phase than isotropic region shows that the molecular packing in the nematic phase and the accompanying growth of long range orientational order from a completely disordered molecular arrangement in the isotropic phase. In 6-Cyano-2-naphthyl 4-heptylcyclohexanecarboxylate the density slopes across different phases are $1.25 \times 10^{-4} \text{C}^{-1}$, $1.4 \times 10^{-4} \text{C}^{-1}$ and $1.6 \times 10^{-4} \text{C}^{-1}$, the value of slopes increases in nematic crystal transition. The higher value of slope in nematic phase than isotropic region indicates that the molecular packing in the nematic phase and the accompanying growth of long range orientational order from a completely disordered molecular arrangement in the isotropic phase. In SmA transition the higher slope of the density variation with temperature than nematic and isotropic suggests an additional packing of molecules with the positional and translational order. The nematic to SmA transition is the situation of nucleation that is the development of translucent, a phase can be visible outwardly at the lower part of the pycnometer bulb that the transparent isotropic liquid seems to float over it with a clear boundary emphasizing the conjunction of two phases. All these transitions are first order nature due to density variations with temperature.

Molecular Polarizabilities

The mean molecular polarizability procured using Lippincott δ function model is $27.34 \times 10^{-24} \text{cm}^3$ and $36.703 \times 10^{-24} \text{cm}^3$. The temperature variation of refractive indices in nematic phase of the compounds are illustrated in Fig.5 and Fig.6. The refractive indices of two compounds are estimated using altered spectrometer appended with small angle prism which houses the liquid crystal sampling. The cell is kept in a heating block for the estimation of refractive indices with temperature. The detachment is clearly seen in the telescope of altered spectrometer at angle of minimum deviation. The refractive index shows small change in isotropic phase and at isotropic nematic phase transformation. The isotropic value splits into two one higher and the other lower than isotropic value corresponding to extraordinary (n_e) and ordinary (n_o) refractive indices respectively. In the nematic region n_e increases while n_o decreases with decrease of temperature and both attain saturation in the deep nematic region. The





Shobha et al.,

birefringence observed in first compound is 0.0967 to 0.1697 and the birefringence in compound two is 0.09671 to 0.22. The ordinary and extraordinary polarizability values are estimated both by Vuk's and Neugebauer methods and which are in nematic phase and illustrated in table 5 and table 6. The mean molecular polarizability by Vuk's method is $24.38 \times 10^{-24} \text{cm}^3$ and $38.63 \times 10^{-24} \text{cm}^3$ for compounds one and two. By Neugebauer method this values are $24.2 \times 10^{-24} \text{cm}^3$ and $38.25 \times 10^{-24} \text{cm}^3$. The molecular polarizabilities obtained by Lippincott δ - function model is sensibly in good understanding with the Vuk's and Neugebauer methods. The values of the polarizabilities are got by various methods are outlined in table 7.

Histogram Equalization

Image enhancement technique brings out the detail in an image that features certain highlights of interest in an image. Enhancement techniques incorporate contrast adjustment, filtering, morphological filtering and deblurring. Image enhancement operations typically return a changed variation of the original image and are habitually used as a preprocessing move to work on the aftereffects of image analysis technique [20]. Fig. 9(a) is the gathered image of the pure compound 4-Cyano-4'-propoxy-1, 1'-biphenyl, Nematic transition at temperature 62°C. It is black and has low dynamic scale in the middle. The low dynamic scale is evident from the way that the width of histogram is narrow with respect to entire gray scale. The image in Fig.9(b) shows the changed image of true Red Green Blue color image of original texture. Fig. 9(c) is the histogram equalized outcome. Fig.10(a) manifests histogram based Red Green Blue concentration. We observe the histogram is concentrated towards blacker side i.e., intensity is fascinated towards the left half of the graph. Fig. 10(b) shows the low contrast RGB image of Fig.9 (b). This is confirmed as low contrast image from the evident that histogram is focused at middle portion in Fig. 10(b), from Fig. 10(c) there is an improvement in average intensity and contrast are noticed. The increase in contrast is because of the extensive spread of the histogram over the whole intensity scale. The increase in overall intensity is because of the way that the average intensity in the histogram of the equalized image is higher than the original. The contrast of the image is improved and it is easy to observe the texture from the acquired images in this methodology. In this work adaptive histogram equalization is utilized to enhance the image standard. Adaptive histogram equalization upgrades on this by transforming each pixel with transformation function derived from neighborhood region. This image enhancement is an extra work which we carried to have a clear picture on the image at transition temperatures to identify the phase without any problem. The image enhancement by histogram equalization is observed in different liquid crystalline phases of compound 4-Cyano-4'-propoxy-1, 1'-biphenyl and 6-Cyano-2-naphthyl 4-heptylcyclohexanecarboxylate in Fig. 11, Fig. 12, Fig. 13 and Fig.14 respectively.

REFERENCES

1. Bahadur, B., (1984). *Mol. Cryst. Liq. Cryst.*, 109(1), 3-93. <https://doi.org/10.1080/00268948408080827>.
2. R.N.V. Ranga Reddy, A. Suryanarayana & V.R. Murthy (1999). *Coefficient of volume expansion and thermoacoustic parameters of alkyl-cyano-biphenyl liquid crystal*, *Cryst. Res. Technol.* 34(10), 1299-1307. [https://doi.org/10.1002/\(SICI\)1521-4079\(199912\)34:10%3C1299::AID-CRAT1299%3E3.0.CO;2-Y](https://doi.org/10.1002/(SICI)1521-4079(199912)34:10%3C1299::AID-CRAT1299%3E3.0.CO;2-Y)
3. B. Gogoi, T.K. Ghosh, & P.R. Alaphati, (2005). *Experimental investigations exhibited by symmetric liquid crystals*, *Cryst. Res. Technol.* 40(7), 709-712. <https://doi.org/10.1002/crat.200410413>
4. B. Gogoi, P.R. Alapati, & A.L. Varama, (2002). *Phase Transition studies in mesogenic dimmers*, *Cryst. Res. Technol.* 37 (12), 1331-1337. <https://doi.org/10.1002/crat.200290010>
5. K. Fakruddin, R. J. Kumar, V.G.K.M. Pisipati, D. Madhavalatha, B.T.P. Madhava, & P.V.D. Prasad, (2010). *Phase transitions and thermodynamic parameters of n-(p-n octyloxybenzylidene)-p-n-alkoxyanilines-A dilatometric study*, *Mol. Cryst. Liq. Cryst.* 524(1), 102-118. <https://doi.org/10.1080/15421406.2010.484614>
6. N. Ajeetha, M. R. N. Rao, P. V. D. Prasad, & V.G.K.M. Pisipati, (2006). *Synthesis, characterization, and dilatometric studies on n-(p-n-alkoxybenzylidene)-p-n-pentyloxyanilines compounds*, *Mol. Cryst. Liq. Cryst.* 457(1), 3-25. <https://doi.org/10.1080/15421400500447108>





Shobha et al.,

7. N. Ajeetha, M. R. N. Rao, P. V. D. Prasad, & V.G.K.M. Pisipati, (2005). *Phase transitions and pre-transitional effects in N-(p-n-pentylbenzylidene)-p-n-pentylaniline (5.5) and its oxygen derivatives – A dilatometric study*, Z. Naturforsch, 60(10), 749-752. https://ui.adsabs.harvard.edu/link_gateway/2005ZNA...60..749A/doi:10.1515/zna-2005-1009
8. Padmaja. S., Ramakrishna nanchara Rao, M, Datta Prasad P.V. & V.G.K.M. Pisipati (2005). *Studies of the Orientational Disorder at the Isotropic Smectic-F Interface*,
9. Z-Naturforsch, 60a, 296-300. <https://doi.org/10.1515/zna-2005-0414>
10. Rao, N.V.S., Potukuchi, D.M., & Pisipati V.G.K.M. (1991). *Phase Transitions in N(p-n-Bu toxybenzylidene) p-n-Alkyl Anilines: Density and Refractive Index Studies*, Mol. Cryst. Liq. Cryst., 196(1), 71-87. <https://doi.org/10.1080/00268949108029688>
11. Pisipati V.G.K.M., (2003). *Polymesomorphism in N-(p-n-Alkoxybenzylidene)-p-n-Alkylanilines (nO.m) Compounds*. Z-Naturforsch, 58a, 661-663. <http://www.znaturforsch.com/aa/v58a/58a0661.pdf>
12. Pisipati V.G.K.M., Rao, N.V.S., Potukuchi, D.M., Alapati, P.R. & Bhaskara Rao, P. (1989). *N-SA Transition First or Second Order: Tricritical Point (TCP) in N(p-n-pentyl oxy benzylidene) p-n-alkyl anilines?*, Mol. Cryst. Liq. Cryst., 167(1), 167-171. <https://doi.org/10.1080/00268948908037172>
13. Rao, N.V.S., & Pisipati V.G.K.M., (1985). *Smectic C to Nematic Phase Transition Studies in NOBA*, Z-Naturforsch, 40a, 466-468. http://zfn.mpdl.mpg.de/data/Reihe_A/40/ZNA-1985-40a-0466.pdf
14. Sharma, B.K. (1980). *Liquid fluorine properties by the hardsphere model with attractive interactions*, Pramana Journal of physics, 14(6), 477-483. <https://www.ias.ac.in/public/Volumes/pram/014/06/0477-0483.pdf>
15. G.R.Luckhurst, B.A.Timini, Pisipati V.G.K.M., & Rao N.V.S., (1985). *The Structure of the Smectic C Phase of 4-n-Heptyl Oxybenzylidene-4'-n-Butylaniline. A Determination of the Core Tilt Angle by Electron Resonance Spectroscopy*, Mol. Cryst. Liq. Cryst. 1(1-2), 45-52. <https://www.tandfonline.com/doi/abs/10.1080/01406566.1985.10766964>.
16. G.W. Gray & G.W. Goodby, (1984). *Smectic Liquid Crystals – Textures and Structures*, Leonard Hill, London, Glassgow. XVI, 162S. <https://doi.org/10.1002/ange.19850970538>
17. C.N.R. Rao & K.J. Rao, (1978). *"Phase transition studies in solids"*, Mc Graw – Hill Inc., U.S.A., 83(10), 1050. <https://doi.org/10.1002/bbpc.19790831022>
18. S. Chandrashekhar & N.V. Madhusudhana, (1969). *Orientational order in p-azoxyanisole, p-azoxyphenetole and their mixtures in the nematic phase*, Journal Physique. Colloq. (paris), C-4., C4-24 - C4-27. <http://hdl.handle.net/2289/4559>
19. H.S. Subramanyam & D. Krishnamurthy, (1973). *Polarization field and molecular order in nematic liquid crystals*, Mol. Cryst. Liq. Cryst., 22(3-4), 239-248. <https://doi.org/10.1080/15421407308083347>
20. J Sivasri, B T P Madhav, M C Rao, & R K N R Manepalli, (2017). *Nano-dispersed Fe₃O₄ liquid crystal compound image enhancement using advanced histogram equalization technique*, Research Journal of Pharmaceutical, Biological and Chemical Sciences. 8(1), 919-928. <https://scholar.google.com/scholar?cluster=17704774870179115383&hl=en&oi=scholar>
21. E.R. Lippincott & J.M. Stutma, (1965). *Polarizabilities from the δ -Function Model of Chemical Binding. II. Molecules with Polar Bonds*, J.Phys.Chem., 70(1), 78. http://lib3.dss.go.th/fulltext/scan_ebook/j.of_physical_1966_v70_n1.pdf

Table: 1 Phase transition temperature and phase variants observed in DSC and Polarizing Optical Microscope.

Compound	DSC/POM	Transition temperature in °C				Thermal Range
		I-N	N-SmA	SmA-Cr	N-Cr	ΔN
C1	DSC	61.89	--	--	53.85	8.04
	POM	62	--	--	52	10
C2	DSC	157.31	103.11	49.77	--	54.2
	POM	159	106	50	--	53





Shobha et al.,

Table:2 Parallel, Perpendicular, Non Bond regions and the Polarizabilities mean of the compounds are assessed by the Lippincott δ function Method & shown in the following table. (10^{-24} Cm³)

Sl. No.	Compound	Parallel Bond component of Polarizability $\alpha_{ }$	Perpendicular Bond component of Polarizability $2\alpha_{\perp}$	Polarizability of Non Bond Region Electrons α_n	Mean Polarizability α_{Mean}
1	C1	56.23	24.961	0.832	27.34
2	C2	65.93	42.94	1.24	36.703

Table: 3 The thermal expansion coefficient, density jump and density slope in different phases of the liquid crystals.

Compound	Phase Variant	% of $(\Delta\rho/\rho)$	α_{I-N} $\times 10^{-4}$ $^{\circ}\text{C}^{-1}$	α_{N-cr} $\times 10^{-4}$ $^{\circ}\text{C}^{-1}$	α_{N-SmA} $\times 10^{-4}$ $^{\circ}\text{C}^{-1}$	$(d\rho/dT)_I$ $\times 10^{-4}$ $^{\circ}\text{C}^{-1}$	$(d\rho/dT)_{N-cr}$ $\times 10^{-4}$ $^{\circ}\text{C}^{-1}$	$(d\rho/dT)_{N-SmA}$ $\times 10^{-4}$ $^{\circ}\text{C}^{-1}$	$(d\rho/dT)_{Cry}$ $\times 10^{-4}$ $^{\circ}\text{C}^{-1}$
C1	I-N	0.1807	7.6	--	--	1.73	--	--	--
	N-Cr	0.129	--	2.35	--	--	5	--	5.2
C2	I-N	0.2054	17.5	--	--	1.25	--	--	--
	N-S	0.122	--	--	9.2	--	--	1.4	--
	SmA-Cry	--	--	--	--	--	--	--	1.6

Table:4 Molecular Polarizability of C1 by Vuk's and Neugebauer Method is shown in the following table. (10^{-24} Cm³)

T °C	Vuk's method (10^{-24})cm ³		Polarizability anisotropy	Neugebauer method (10^{-24})cm ³		Polarizability anisotropy
	α_e	α_o	$\Delta\alpha=\alpha_e - \alpha_o$	α_e	α_o	$\Delta\alpha=\alpha_e - \alpha_o$
53.5	31.63958	20.04438	11.5952	30.4714	20.62847	9.84293
54	31.59269	20.08562	11.50706	30.43148	20.66623	9.765254
54.5	31.57046	20.13696	11.4335	30.41417	20.7151	9.699066
55	31.51496	20.17646	11.3385	30.36646	20.75071	9.615753
55.5	31.4643	20.20628	11.25802	30.32264	20.77711	9.545532
56	31.44358	20.24457	11.19901	30.30609	20.81331	9.492774
56.5	31.39387	20.29279	11.10108	30.26397	20.85774	9.406233
57	31.33367	20.30338	11.0303	30.21068	20.86487	9.345808
57.5	30.93491	20.16249	10.77241	29.83371	20.71309	9.120622
58	31.12028	20.56323	10.55704	30.03171	21.10752	8.924196
58.5	30.99878	20.7954	10.20338	29.93388	21.32785	8.606029
59	30.73678	21.11354	9.623245	29.71387	21.62499	8.088882
59.5	30.56778	21.31144	9.256338	29.57161	21.80953	7.762077
60	30.37091	21.56228	8.808629	29.40666	22.0444	7.362264
60.5	30.02529	22.00052	8.024775	29.11601	22.45516	6.660851
61	29.58898	22.63059	6.958383	28.74978	23.05019	5.699591
61.5	29.31812	22.73534	6.582785	28.50719	23.14081	5.366381

Table:5 Molecular Polarizability of C2 by Vuk's and Neugebauer Method is shown in the following table. (10^{-24} Cm³)

T °C	Vuk's method (10^{-24})cm ³		Polarizability anisotropy	Neugebauer method (10^{-24})cm ³		Polarizability anisotropy
	α_e	α_o	$\Delta\alpha=\alpha_e - \alpha_o$	α_e	α_o	$\Delta\alpha=\alpha_e - \alpha_o$



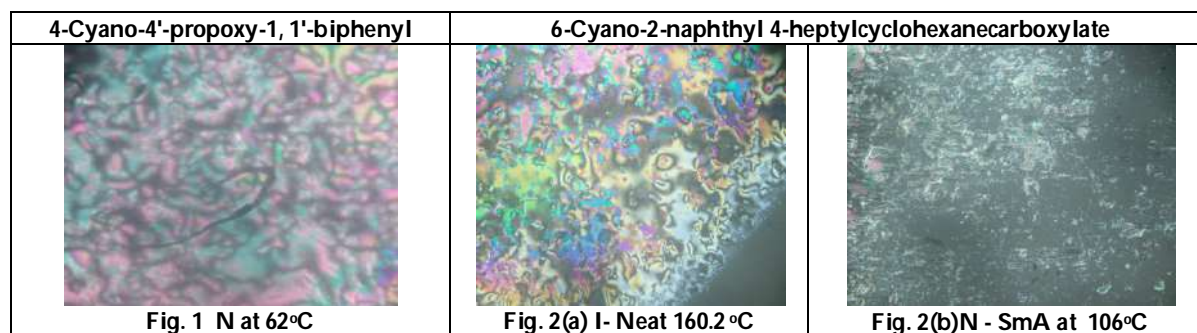


Shobha et al.,

103	54.42086	30.20175	24.2191	52.08274	31.37082	20.71192
105	54.43639	30.21037	24.22601	52.0976	31.37977	20.71783
107	54.45192	30.21899	24.23293	52.11247	31.38872	20.72374
109	54.50738	30.24977	24.25761	52.16554	31.42069	20.74485
111	54.20213	30.25735	23.94478	51.89195	31.41244	20.4795
113	53.89338	30.29989	23.59349	51.61809	31.43753	20.18056
115	53.75498	30.41553	23.33945	51.49916	31.54344	19.95572
117	53.33934	30.66161	22.67773	51.13716	31.7627	19.37446
119	52.99481	30.75155	22.24325	50.83292	31.8325	19.00043
121	52.77923	30.86744	21.91179	50.64508	31.93452	18.71056
123	52.56461	30.97643	21.58817	50.45783	32.02983	18.428
125	52.19662	31.27662	20.92	50.14101	32.30443	17.83658
127	51.98318	31.38678	20.5964	49.95494	32.40091	17.55403
129	51.74623	31.58786	20.15837	49.75166	32.58514	17.16651
131	51.43788	31.81424	19.62364	49.48663	32.78987	16.69676
133	51.06625	32.00655	19.05971	49.16121	32.95907	16.20214
135	50.86076	32.11679	18.74397	48.98225	33.05605	15.9262
137	50.59783	32.32075	18.27707	48.75593	33.2417	15.51423
139	50.4178	32.66937	17.74843	48.61083	33.57286	15.03798
141	50.33987	32.8101	17.52977	48.54791	33.70607	14.84184
143	50.0778	33.08973	16.98808	48.32612	33.96557	14.36054
145	49.88397	33.46445	16.41952	48.17031	34.32128	13.84903
147	49.46403	33.97755	15.48648	47.81788	34.80062	13.01726
149	49.19462	34.29783	14.8968	47.59142	35.09943	12.49199
151	48.87853	34.70204	14.17649	47.32669	35.47796	11.84873
153	48.32393	35.40853	12.9154	46.8605	36.14025	10.72025
155	47.62331	36.42383	11.19948	46.27263	37.09917	9.173464
157	47.28012	36.66434	10.61578	45.97236	37.31822	8.65414

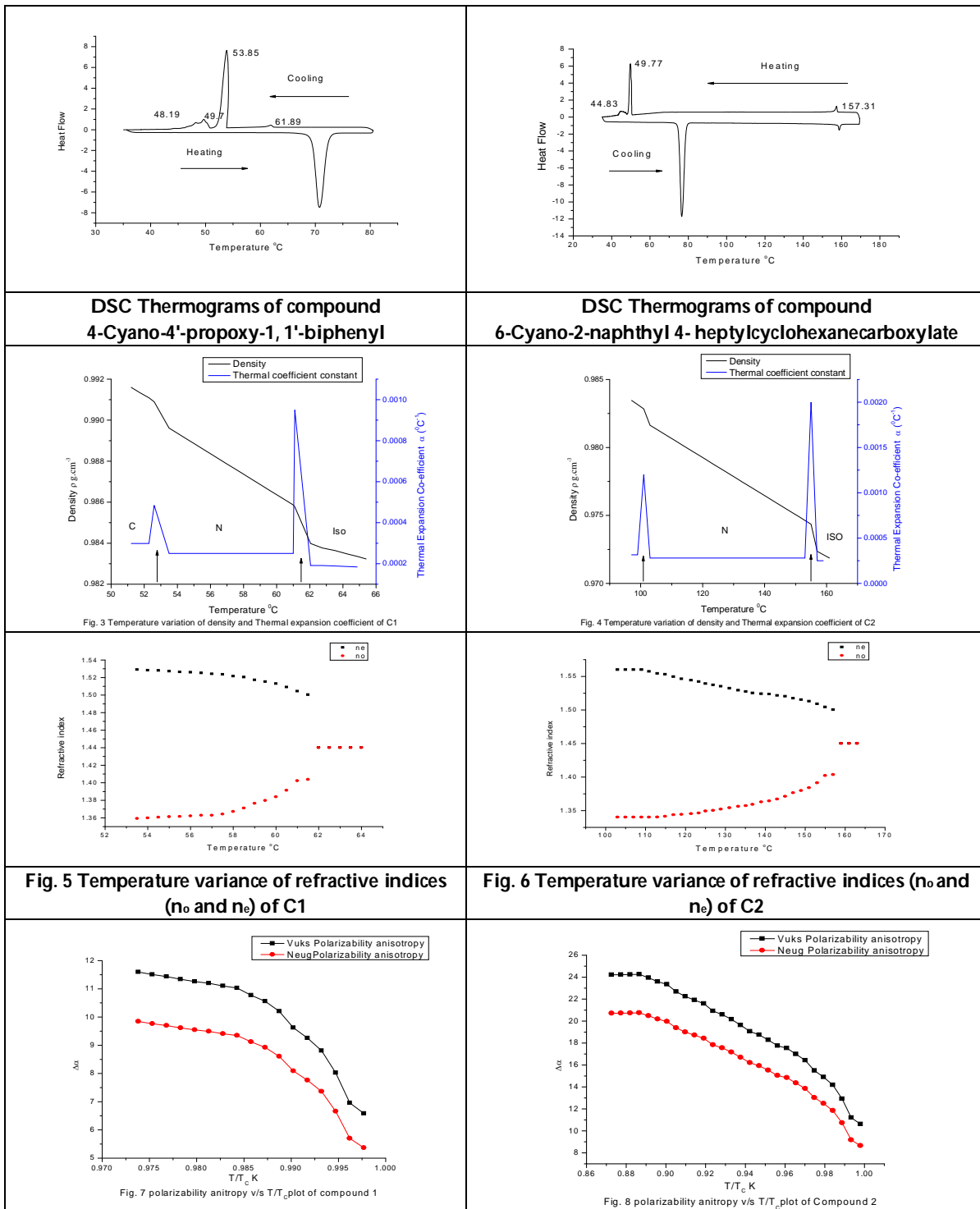
Table:6 The molecular polarizabilities of the compounds measured by both theoretical and experimental Methods

Compounds	Theoretical Method		Experimental Methods	
	Lippincott δ -Function method (10^{-24})cm ³		Vuk's Method (10^{-24})cm ³	Neugebauer Method (10^{-24})cm ³
C1	27.34		24.38	24.2
C2	36.703		38.63	38.25





Shobha et al.,





Shobha et al.,

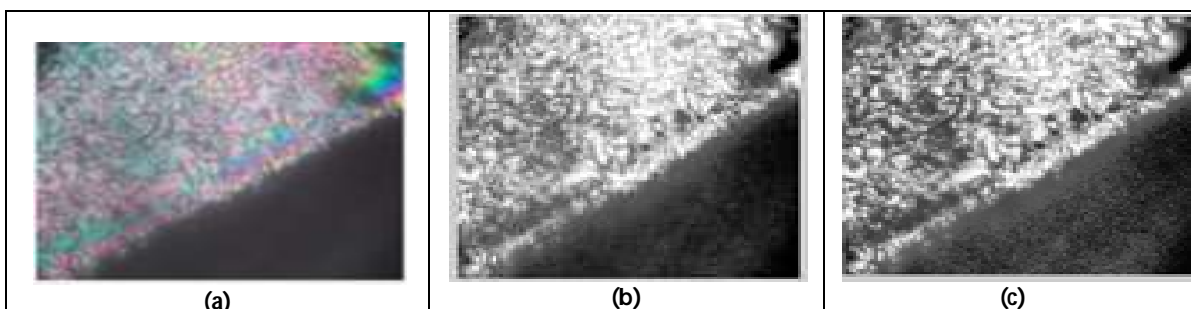


Fig. 9(a): Original texture of compound 1 at 62°C obtained by thermal microscope (2437 x 1919 pixels),
9(b): Histogram equalized Red Green Blue color image of original texture,
9(c): Histogram equalized Red Green Blue color image with contrast enhancement.

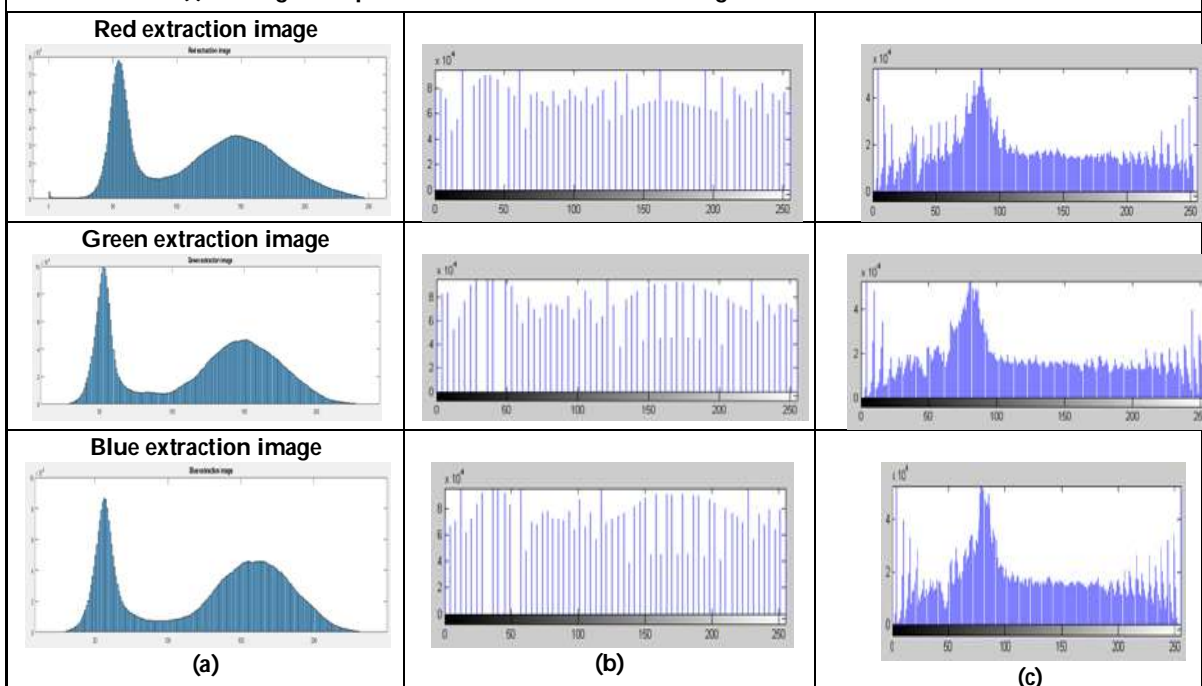


Fig. 10(a): Histogram- based RGB concentration **10(b):** Histogram equalized RGB concentration of 10(a),
10(c): Adaptive Histogram RGB concentration of 10(b),

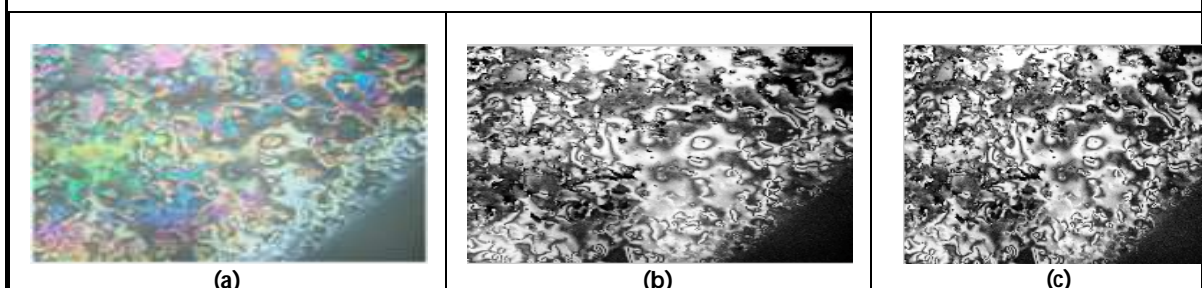
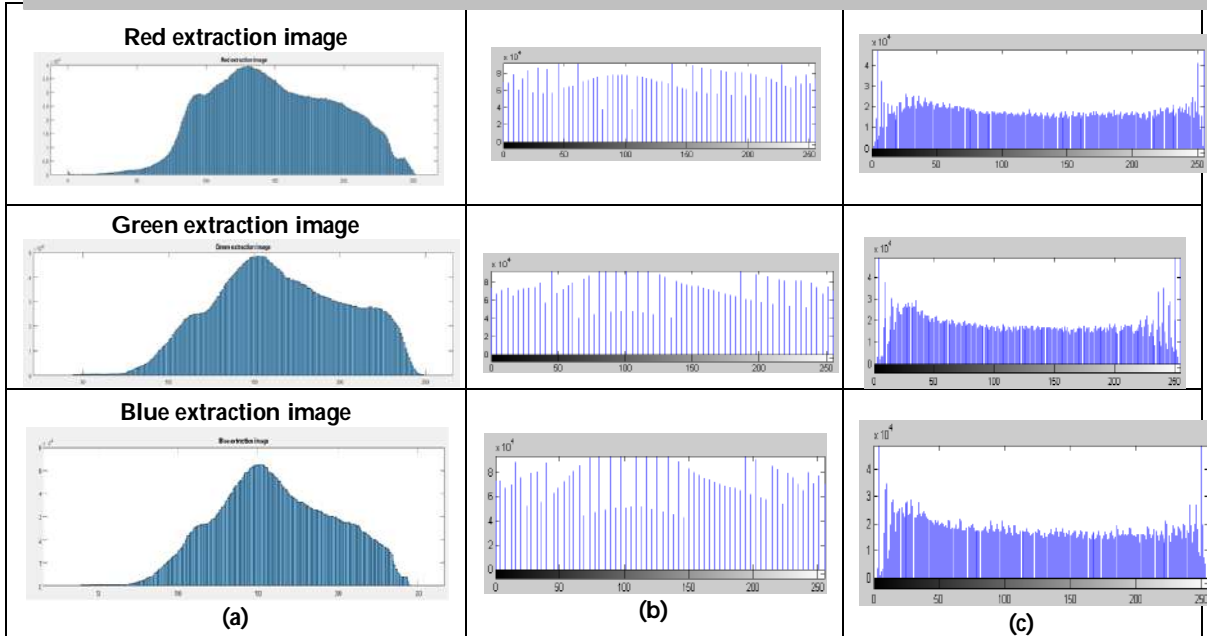


Fig.11(a):Original texture of compound 2 at 160.2 °C obtained by thermal microscope(2437 x 1919 pixels),
11(b):Histogram equalized Red Green Blue color image of original texture,
11(c):Adaptive Histogram Red Green Blue color image with contrast enhancement.





Shobha et al.,



**Fig. 12(a): Histogram- based RGB concentration
 12(b): Histogram equalized RGB concentration of 12(a),
 12(c): Adaptive Histogram RGB concentration of 12(b),**

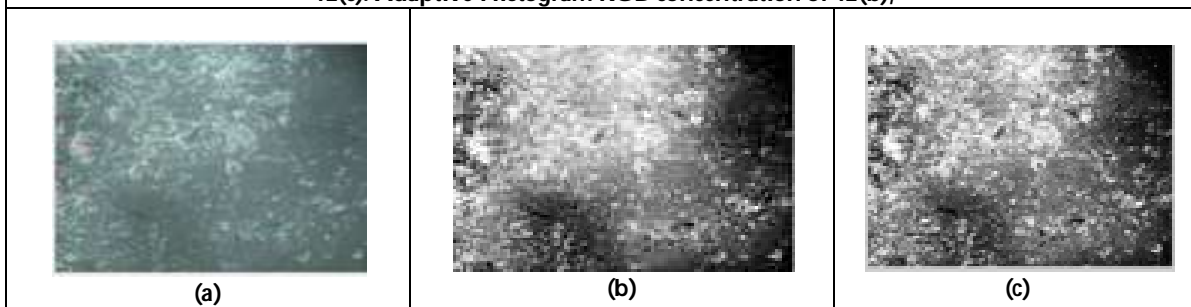
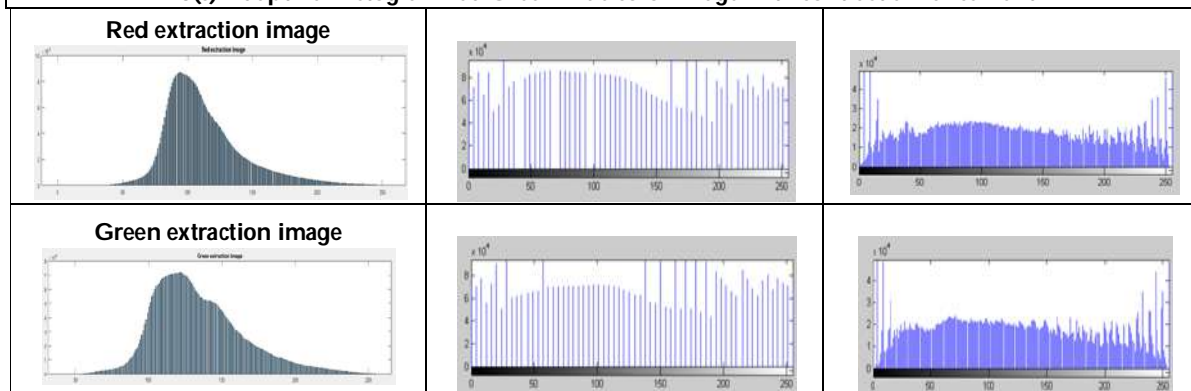


**Fig.13(a): Original texture of compound 2 at 106 °C obtained by thermal microscope (2437 x 1919 pixels),
 13(b):Histogram equalized Red Green Blue color image of original texture,
 13(c):Adaptive HistogramRed Green Blue color image with contrast enhancement.**





Shobha et al.,

